

26. Vooijs, M., Jonkers, J., Lyons, S., and Bernes, A. (2002) Noninvasive imaging of spontaneous retinoblastoma pathway-dependent tumors in mice. *Cancer Res* 62, 1862–1867.
27. Lyons, S.K. (2005) Advances in imaging mouse tumor models in vivo. *J Pathol* 205, 194–205.
28. Laurie, N.A., Gray, J.K., Zhang, J., Leggas, M., Relling, M., Egorin, M., Stewart, C., and Dyer, M.A. (2005) Topotecan combination chemotherapy in two new rodent models of retinoblastoma. *Clin Cancer Res* 11, 7569–7578.
29. Takeshita, F., Bader, A.G., Osaki, M., Takahashi, R., Yamamoto, Y., Kosaka, N., Kawamata, M., Kelnar, K., Brown, D., and Ochiya, T. (2010) Systemic delivery of miR-16 for RNAi therapy in prostate cancer. *Mol Ther* 18, 181–187.

Micromanaging Iron Homeostasis

HYPOXIA-INDUCIBLE MICRO-RNA-210 SUPPRESSES IRON HOMEOSTASIS-RELATED PROTEINS^{*[5]}

Received for publication, February 27, 2012, and in revised form, August 14, 2012. Published, JBC Papers in Press, August 15, 2012, DOI 10.1074/jbc.M112.356717

Yusuke Yoshioka^{*§1}, Nobuyoshi Kosaka[§], Takahiro Ochiya[§], and Takashi Kato^{*¶2}

From the ^{*}Integrative Bioscience and Biomedical Engineering, Graduate School of Science and Engineering, Waseda University, 2-2 Wakamatsu, Shinjuku, Tokyo 162-8480, Japan, the [§]Translational Research Group Division of Molecular and Cellular Medicine, National Cancer Center Research Institute, 5-1-1 Tsukiji, Chuo-ku, Tokyo 104-0045, Japan, and the [¶]Department of Biology, School of Education, Waseda University, Tokyo 162-8480, Japan

Background: The regulatory mechanisms of iron homeostasis in cancer cells are not yet fully understood.

Results: MicroRNA-210 suppresses two essential molecules for iron homeostasis, TfR and ISCU.

Conclusion: Precise regulation of microRNA-210 expression level is vital for maintaining the iron homeostasis, leading to the survival of cancer cells.

Significance: This study reveals the linkages among hypoxia, iron homeostasis, and cancer.

Iron is fundamental for sustaining life for living organisms, and the iron metabolism is finely regulated at different levels. In cancer cells, deregulation of the iron metabolism induces oxidative stress and drives tumor progression and metastasis; however, the molecular mechanisms of iron homeostasis are not fully understood. Here we found that iron deficiency as well as hypoxia promoted microRNA-210 (miR-210) expression. A central mediator of miR-210 transcriptional activation is the hypoxia-inducible factor (HIF)-1 α , and the hypoxia-response element in the miR-210 promoter is confirmed experimentally. This is in agreement with the data from *in vivo* studies that have demonstrated the presence of miR-210-expressing cells at the chronic hypoxic regions of xenografted tumors. Furthermore we found two essential molecules for iron homeostasis, iron-sulfur cluster scaffold protein (ISCU) and transferrin receptor 1 (TfR), are a direct target of miR-210. Transfection of miR-210 decreases the uptake of transferrin by inhibiting the expression of TfR. In addition, inhibition of miR-210 by anti-miR-210 up-regulates ISCU expression. These findings suggest that miR-210 works as an iron sensor and is involved in the maintenance of iron homeostasis by sustaining the TfR expression level to stimulate cell proliferation and promote cell survival in the hypoxic region within tumors.

During the evolutionary processes, life has made use of iron in a variety of biochemical processes. For instance, iron is an essential cofactor for nonheme enzymes, such as ribonucleotide reductase, which is essential for DNA synthesis and is also a vital component of the heme in the oxygen-binding protein, hemoglobin (1–3). Iron needs to be tightly regulated, as excess iron is toxic and causes the generation of free radicals (4), whereas iron insufficiency induces hypoferric anemia in mammals (5) coupled to hypoxia in tissues (6, 7). Given the links between iron metabolism and oxygen transport, the associations between the control of the iron concentration and the physiology of the hypoxic response are important (8). Many responses to altered oxygen levels are coordinated by a hypoxia-inducible factor (HIF)³ (9, 10).

The association between iron and cancer has been shown in animal models and epidemiologic studies in several human cancers. For instance, the oldest reported experiment of iron-induced carcinogenesis is that of mice exposed to iron-oxide dust, which caused pulmonary tumors (11). In addition, various studies have also shown higher levels of expression of the transferrin receptor 1 (TfR), which is an essential protein involved in iron uptake and the regulation of cell growth, in cancer cells than in their normal counterparts (12). TfR could be attributed to the increased need for iron as a cofactor of ribonucleotide reductase involved in the DNA synthesis of rapidly dividing cells. These reports suggest that iron homeostasis is important in cancer initiation and progression. However, the regulatory mechanisms of iron homeostasis in cancer cells are not yet fully understood.

MicroRNAs (miRNAs) have emerged as a new class of non-coding genes involved in regulating a wide variety of biological processes (13, 14), and their mis-expression has been shown to contribute to tumorigenesis (15). Therefore, miRNAs act as

^{*}This work was supported in part by a grant-in-aid for the third-term comprehensive 10-year strategy for cancer control, a grant-in-aid for scientific research on priority areas cancer from the Ministry of Education, Culture, Sports, Science, and Technology, and the Program for Promotion of Fundamental Studies in Health Sciences of the National Institute of Biomedical Innovation (NiBio), the Japan Society for the Promotion of Science (JSPS) through the "Funding Program for World-Leading Innovative R&D on Science and Technology (FIRST Program)," initiated by the Council for Science and Technology Policy (CSTP). This work was supported in part by a grant from the Japan Society for the Promotion of Science (to Y. Y.).

[§]This article contains supplemental Figs. S1–S7.

¹Supported by a Research Fellowship of the Japan Society for the Promotion of Science for Young Scientists.

²To whom correspondence should be addressed: Department of Biology, School of Education and Molecular Physiology Unit Major in Integrative Bioscience and Biomedical Engineering, Graduate School of Science and Engineering, 2-2 Wakamatsu, Shinjuku, Tokyo 162-8480, Japan. Tel.: 81-3-5369-7309; Fax: 81-3-3355-0316; E-mail: tkato@waseda.jp.

³The abbreviations used are: HIF, hypoxia-inducible factor; Tf, transferrin; TfR, transferrin receptor 1; miRNA, microRNA; miRNA-210, microRNA-210; ISCU, iron-sulfur cluster scaffold protein; DFO, desferrioxamine; qRT-PCR, quantitative real-time RT-PCR; IRP1, iron regulatory protein 1; NC, negative control.

tuners of gene expression and maintain homeostasis. For instance, miR-144/451 knockout mice display a cell autonomous impairment of late erythroblast maturation, resulting in erythroid hyperplasia, splenomegaly, and mild anemia (16).

In a previous report, we demonstrated that miR-210 is highly expressed in human and murine erythroid cells and in the spleen of mice with hemolytic anemia (17). Erythrocytes require iron to perform their duty as oxygen carriers. Recent reports have shown that the expression of miR-210 is induced by hypoxic conditions (18). Therefore, miR-210 might play an important role in the connection of iron and oxygen. It was already reported that the expression of miR-210 was tightly associated with poor prognosis of breast cancer (18); however, contradictory data exist concerning the regulation and roles of miR-210 during cancer progression. In this study, we clarified that miR-210 regulates iron homeostasis in cancer cells. The expression of miR-210 was induced not only in hypoxic conditions but also in iron deficiency. In addition, we found that the targets of miR-210 are two essential molecules for iron homeostasis, TfR and the iron-sulfur cluster scaffold protein (ISCU). Furthermore, we showed that the distribution of miR-210-expressing cells in inoculated tumor cells could be observed in the chronic hypoxic regions. These results indicated that iron-deficiency-inducible miR-210 controls the expression of two iron regulatory proteins to optimize the survival and proliferation rate of cancer cells located in the chronic hypoxic regions.

EXPERIMENTAL PROCEDURES

Reagents—Rabbit polyclonal anti-ISCU (FL-142) (sc-28860) was purchased from Santa Cruz Biotechnology (Santa Cruz, CA). Mouse monoclonal anti-TfR (13-6800) was purchased from Invitrogen. Mouse monoclonal anti-actin, clone C4 (MAB1501), was purchased from Millipore (Billerica, MA). Mouse monoclonal anti-HIF-1 α (610959) was purchased from BD Biosciences. Rabbit monoclonal anti-ferritin (EPR3004Y) was purchased from Epitomics (Burlingame, CA). Rabbit polyclonal anti-ACO1/iron regulatory protein 1 (IRP1) was purchased from Medical & Biological Laboratories Co., Ltd. Rabbit polyclonal anti-red fluorescent protein (ab34771) was purchased from Abcam (Cambridge, MA). Peroxidase-labeled anti-mouse and anti-rabbit antibodies were included in the Amersham Biosciences ECL Plus Western blotting reagents pack (RPN2124) (GE Healthcare). Synthetic hsa-miR-210 (pre-miR-210) and antisense miR-210 oligonucleotide (anti-miR-210) were purchased from Ambion (Austin, TX). The duplexes of each small interfering RNA (siRNA) targeting human HIF-1 α mRNA (s30925; target sequences of 5'-GGAGGU-GUUUGACAAGCGAdTdT-3' and 5'-UCGCUUGUCAA-CACCUCCtg-3'), an siRNA-specific for human IRP1 (ACO1) mRNA (target sequences of 5'-GCUCGCUACUUAACUAA-CAtt-3' and 5'-UGUUAGUUAAGUAGCGAGCag-3') and negative control 1 (NC1) were purchased from Applied Biosystems. An siRNA-specific for human TfR mRNA (target sequences of 5'-GAACCUUGGAUUAUGAUGAAAdTdT-3' and 5'-UUCAUCAUUAUCCAGGUUCdTdT-3') was purchased from Sigma-Genosys. Desferrioxamine (DFO) was purchased from Calbiochem. Geneticin was purchased from Invitrogen.

Cell Culture—MCF7 cells and MD-MB-231-luc-D3H2LN cells (Xenogen), a human breast cancer cell line, were cultured in RPMI 1640 medium containing 10% heat-inactivated fetal bovine serum (FBS) and an antibiotic-antimycotic (Invitrogen) at 37 °C in 5% CO₂.

Exposure to Hypoxia—Cells were exposed for 24 h or 48 h either to standard nonhypoxic cell culture conditions (20% O₂, 5% CO₂ at 37 °C) or to hypoxia (1% O₂, 5% CO₂ with N₂ balance at 37 °C) in either a modular hypoxia chamber (Wakenyaku) or a tissue culture incubator.

RNA Extraction—RNA was isolated using TRIzol (Invitrogen) and processed according to the manufacturer's instructions.

Quantitative Real-time RT-PCR (qRT-PCR)—Hsa-miR-210 and endogenous control RNU6B TaqMan qRT-PCR kits and human-ISCU, human-TfR, and human- β -actin TaqMan Gene Expression Assays were purchased from Applied Biosystems (Foster City, CA). The reverse transcription and TaqMan quantitative PCR were performed according to the manufacturer's instructions. PCR was carried out in 96-well plates using the 7300 Real-Time PCR System (Applied Biosystems). All reactions were done in triplicate.

The expression levels of pri-miR-210 and β -actin were measured by qRT-PCR using a SYBR Green PCR Master Mix (Invitrogen). Primer sequences are as follows (shown 5' to 3'): pri-miRNA-210_F, GACTGGCCTTTGGAAGCTCC and R, ACAGCCTTCTCAGGTGCAG; β -actin_F, GGCACCAC-CATGTACCCTG and R, CACGGAGTACTTGCGCTCAG.

In Silico MicroRNA Target Prediction—Bioinformatic prediction of target genes and miRNA-binding sites was performed using three programs: TargetScan (version 5.0) (19), Sanger miRBase (version 5) (20), and MirTarget2 (21).

3'-UTR Assay Plasmid Constructs—A 297-bp fragment from the 3'-UTR of ISCU containing the predicted target sequence of miR-210 (located at positions 102–109 of the ISCU/2 3'-UTR) and a 385-bp fragment from the 3'-UTR of TfR containing the predicted target sequence of miR-210 (located at positions 229–235 of this fragment) were PCR-cloned from MCF7-isolated total RNA. Three prime A-overhang was added to the PCR products after 15 min of regular Taq polymerase treatment at 72 °C. The PCR products were cloned into a pGEM-T Easy Vector (Promega; Madison, WI). A pair of primers including XhoI and NotI restriction sites was designed to amplify the 3'-UTR of ISCU and TfR insert. The amplified products were ligated into the XhoI and NotI sites of the 3'-UTR of the *Renilla* luciferase gene in the psi-check-2 plasmid (Promega) to generate psi-ISCU and psi-TfR. Primer sequences are as follows (shown 5' to 3'): ISCU_F, GCTCGA-GTAACTCCGTTACTTCCAGCAGGC and ISCU_R, GCGG-CCGCTAATATGCACTTCACGGGCTATC; TfR_F, GCTC-GAGTAATCAGCTGTTTGTTCATAGGGC and TfR_R, GCG-GCCGCTAGGTCATGCACGATTGTCCGA. Site-directed mutagenesis or deletion mutant was performed in the seed sequences of ISCU and TfR. PrimeStar Max DNA Polymerase (Takara; Kyoto, Japan) was used for PCR amplification. Forward primer and reverse primer sequences are as follows (shown 5' to 3'): ISCU_mut_F, AGATGTATGTGGTACTTGTCTGTTACGTTA and ISCU_mut_R, GTACCACATACAT-

Regulation of Iron Homeostasis by miR-210

CTCATAGCTCTTCGGT; ISCU_del_F, ATGAGATTACTT-GCTGTTACGTTA and ISCU_del_R, GCAAGTAATCTC-ATAGCTCTTCGGT; Tfr_mut_F, TGTTGCACGCGCGTA-CTTAAATGAAAGCA and Tfr_mut_R, TACGCGCGTGCA-ACACCCGAACCAGGAAT; Tfr_del_F, CGGGTGTTTCGT-ACTTAAATGAAAGCA and Tfr_del_R, AAGTACGAACA-CCCGAACCAGGAAT.

Immunoblot Analysis—SDS-PAGE gels were calibrated with Precision Plus Protein standards (161-0375) (Bio-Rad), and anti-HIF-1 α (1:500), anti-ISCU (1:200), anti-Tfr (1:500), and anti-actin (1:1000) were used as primary antibodies. The dilution ratio of each antibody is indicated in parentheses. Two secondary antibodies (peroxidase-labeled anti-mouse and anti-rabbit antibodies) were each used at a dilution of 1:10,000. Bound antibodies were visualized by chemiluminescence using the ECL Plus Western blotting detection system (RPN2132) (GE Healthcare), and luminescent images were analyzed with a LuminoImager (LAS-3000; Fuji Film Inc.).

Flow Cytometric Analysis—MCF7 cells and MDA-MB-231-luc-D3H2LN cells were transfected with pre-miR-210 or pre-NC. After culturing for 48 h, transfected cells were serum-starved for 30 min and then incubated for 45 min in a serum-free medium containing 50 μ g of transferrin/ml conjugated with Alexa Fluor 594 (Invitrogen). Transfected cells were suspended in their culture medium and subjected to a FACSAria II cell sorter (BD Biosciences). At least one million cells were pelleted by centrifugation at 180 \times g for 5 min at 4 $^{\circ}$ C, resuspended in a 20 μ l of a monoclonal mouse anti-human CD71-FITC antibody (BD Biosciences, clone M-A712), and incubated for 30 min at 4 $^{\circ}$ C. Three independent experiments were performed.

Transferrin-uptake Analysis—Transferrin-uptake experiments were performed 48 h after transfection with pre-miR-210 or pre-NC. Transfected cells were serum-starved for 30 min and then incubated for 45 min in a serum-free medium containing 50 μ g of transferrin/ml conjugated with Alexa Fluor 594. Cells were then washed and fixed in 4% paraformaldehyde for 15 min at room temperature. After washing with PBS, they were incubated with mouse anti-Tfr antibody diluted 1:100 in Dako REAL Antibody Diluent (Dako; Carpinteria, CA) for 1 h. They were then incubated with Alexa Fluor 488 goat anti-mouse IgG diluted 1:1000 in Dako REAL Antibody Diluent for 45 min. Finally, the cells were stained with the fluorescent DNA-binding dye Hoechst 33342 (Invitrogen) for 5 min.

Establishment of Stable Cell Lines—Stable knockdown of ISCU MCF7 cell lines was generated by selection with 4 μ g/ml blasticidine (Invitrogen). MCF7 cells were transfected with 0.5 mg of a siISCU1/2 vector or a negative control vector at 90% confluence in 24-well dishes using a Lipofectamine LTX reagent in accordance with the manufacturer's instructions. After 24 h, the cells were replated in a 10-cm dish followed by 3-week selection with 4 μ g/ml blasticidine.

Immunohistochemical Staining—Between all consecutive steps of the staining procedure, the sections were rinsed three times for 5 min in PBS. The sections were first fixed in 10% formalin for 4 h. After re-hydration of the tissue sections in PBS for 1 h, they were incubated with mouse anti-HIF-1 α diluted 1:500 and rabbit anti-red fluorescent protein diluted 1:100 in Dako REAL Antibody Diluent for 1 h. Sections were then incu-

bated with Alexa Fluor 488 goat anti-mouse IgG and Alexa Fluor 594 goat anti-rabbit IgG (Molecular Probes; Leiden, The Netherlands) diluted 1:1000 in Dako REAL Antibody Diluent for 45 min. Finally, sections were mounted on ProLong Gold antifade reagent with DAPI (Invitrogen).

In Vivo miR-210-monitoring Assay—The pDsRed-Express-DR vector (Clontech Laboratories), which is a promoterless vector that encodes DsRed-Express-DR, was purchased from Takara Bio. This protein is a destabilized variant of the red fluorescent protein. For miR-210 promoter-driven fluorescent-based reporter assays, pmiR-210-DsRed was constructed by inserting a miR-210 promoter region into a multi-cloning site of pDsRed-Express-DR vector at HindIII and XhoI sites. A sensor vector for miR-210 was constructed by introducing tandem binding sites with a perfect complementarity sequence to miR-210, separated by a four-nucleotide spacer into the NotI site of pDsRed-Express-DR vector, which already introduced the CMV promoter into the multi-cloning site. The sequences of the binding site are as follows: 5'-AGTGATTACGCCGCTG-TCACACGCACAGACGCGTTACGCCGCTGTACACGC-ACAGATCGAA-3' (sense) and 5'-TTCGATCTGTGCGTGTGACAGCGGCTGAACGCGTCTGTGCGTGTGACAGC-GGCTGAATCACT-3' (antisense). The seed sequence of miR-210 is indicated in bold italics. All plasmids were verified by DNA sequencing.

Statistical Analysis—Data presented as *bar graphs* are the means \pm S.E. of at least three independent experiments. Statistical analysis was performed using Student's *t* test.

RESULTS

Iron Deficiency Induces the Expression of miR-210 through the HIF-1 α , and miR-210 Directly Suppresses ISCU—To try to determine the possible contribution of miR-210 in the regulation of iron homeostasis, we first measured the expression of miR-210 in breast cancer cells, MCF7 and MDA-MB-231 (MM231) cells, and human breast epithelial cells, MCF10A, after treatment with an iron chelator, DFO. The expression level of miR-210 was increased 3–5-fold above basal levels by the 48 h of DFO treatment compared with untreated cells (Fig. 1A). In addition, excess amounts of iron by addition of 500 mM ferric ammonium citrate had no effect on the induction or suppression of the expression of miR-210. To further analyze whether the biogenesis of miR-210 during iron depletion is regulated by a transcriptional mechanism or processing machinery of miRNA biogenesis, we quantified the expression of primary miR-210 (pri-miR-210) in MCF7 cells. The expression of pri-miR-210 levels was induced 1.5–3.5-fold above basal levels by the DFO treatment compared with untreated cells (Fig. 1B). This result indicated that the induction of miR-210 is because of transcriptional regulation. As shown previously, the transcription of miR-210 was regulated by iron-deficient-induced HIF-1 α through the binding of hypoxia-responsible elements that are located upstream of the miR-210 gene (22) (supplemental Fig. S1, A–D). Indeed, suppression of HIF-1 α by siRNA (supplemental Fig. S1E) leads to a significant reduction of miR-210 expression after treatment with DFO (Fig. 1C).

Recent reports showed that miRNAs play a role in feedback and feed-forward transcriptional regulation (23, 24). Previ-

Regulation of Iron Homeostasis by miR-210

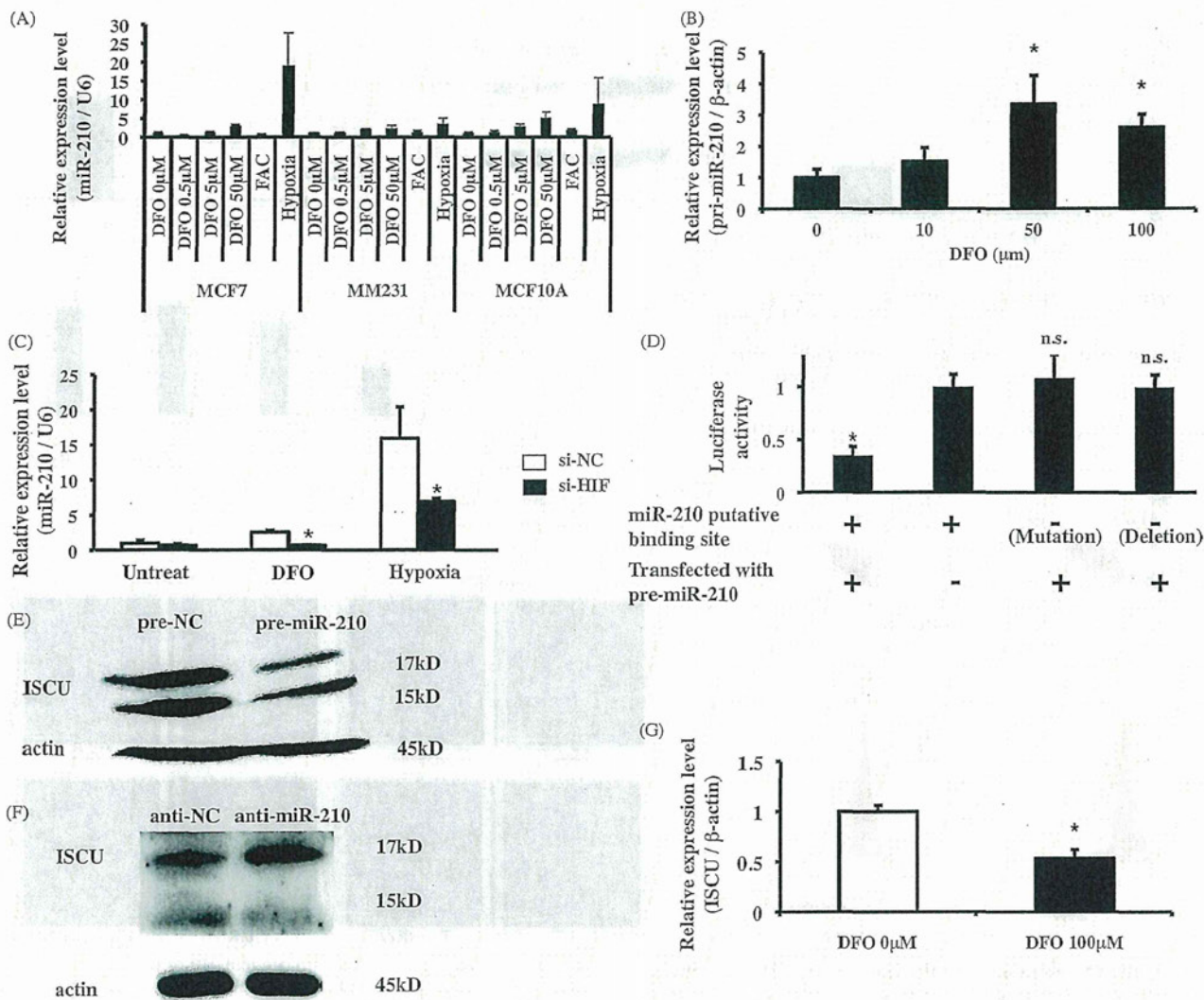


FIGURE 1. Expression of miR-210 is induced by iron deficiency, and target gene of miR-210 is ISCU. *A*, miR-210 expression was detected by qRT-PCR after treatment with various concentrations of DFO or exposure to 1% O₂ for 48 h. RNU6B was used as a control. *B*, primary miR-210 expression was detected by qRT-PCR after treatment with DFO for 48 h. β-Actin was used as a control. *C*, MCF7 cells were transfected with HIF-1α siRNA or control siRNA and treatment with DFO 50 μM or exposure to 1% O₂ for 24 h. miR-210 expression was detected by qRT-PCR. RNU6B was used as a control. *, *p* < 0.05 compared with control siRNA groups. *D*, MCF7 cells were co-transfected with pre-miR-210 or pre-NC and psi-ISCU or with its mutant or deletion vector. After 48 h, luciferase activities were measured. *, *p* < 0.05 compared with pre-NC. *n.s.*, not significant. *E*, MCF7 cells were transfected with pre-miR-210 or pre-NC. After 48 h, ISCU expression was detected by immunoblotting. Actin was used as a loading control. *F*, MCF7 cells were transfected with anti-miR-210 or anti-NC and exposed to 1% O₂. After 48 h, ISCU expression was detected by immunoblotting. Actin was used as a loading control. *G*, ISCU expression was detected by qRT-PCR after treatment with DFO 100 μM for 48 h. *, *p* < 0.05 compared with untreated cells. β-Actin was used as a control.

ously, we reported that miR-210 is involved in the production of erythrocytes, which consume 70% of body iron in humans and are the major carriers of oxygen (17, 25). Based on those reports and our finding that the expression of miR-210 was regulated by the iron concentration through the activation of HIF-1α in this study (Fig. 1, A–C, and supplemental Fig. S1), we hypothesized that miR-210 regulates genes that are associated with a potent iron homeostasis and a hypoxic cellular response. According to these criteria, ISCU was predicted as a miR-210 target by miRNA target prediction algorithm programs (supplemental Fig. S2A). ISCU is an essential factor of the mitochondria electron transport chain, and loss of function of ISCU can disrupt iron homeostasis (26). Although ISCU was known to be regulated by miR-210 in hypoxic condition (27, 28), the precise mechanism of miR-210 on iron homeostasis in cancer cells has

not been clarified yet. As shown in Fig. 1D, miR-210 recognized the 3'-UTR of ISCU. On the contrary, miR-210 seed sequence in the 3'-UTR of ISCU was mutated or deleted, miR-210 could not bind to the 3'-UTR of ISCU (Fig. 1D). In addition, overexpression or knockdown of miR-210 in MCF7 cells down-regulated or up-regulated the expression of ISCU assessed by qRT-PCR (supplemental Fig. S2, C and D) and immunoblotting (Fig. 1, E and F). These results are consistent with previous findings that ISCU was a direct target of miR-210. To understand the contribution of miR-210 and ISCU on iron homeostasis in breast cancer cells, we checked the expression of ISCU under the condition of iron depletion in breast cancer cells. As shown in Fig. 1G, the expression of ISCU was down-regulated after the treatment with DFO, suggesting that the expression of ISCU was controlled by iron-deficient-induced miR-210 in breast

Regulation of Iron Homeostasis by miR-210

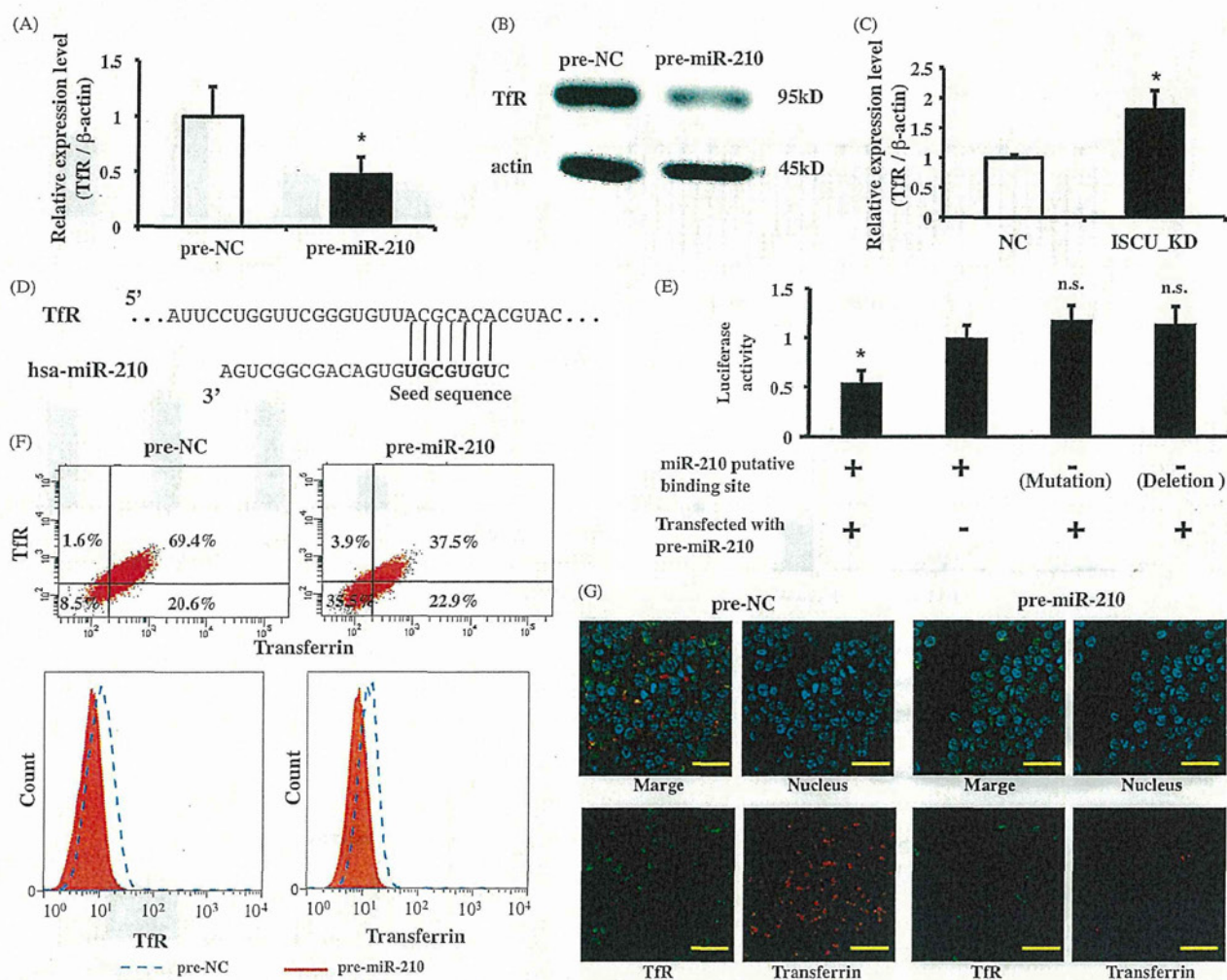


FIGURE 2. miR-210 also represses the expression of TfR as a target gene. A, MCF7 cells were transfected with pre-miR-210 or pre-NC. After 48 h, TfR expression was detected by qRT-PCR. β -Actin was used as a control. *, $p < 0.05$ compared with pre-NC. B, MCF7 cells were transfected with pre-miR-210 or pre-NC. After 48 h, TfR expression was detected by immunoblotting. Actin was used as a loading control. C, expression of TfR is increased by knockdown of ISCU. TfR expression was detected in ISCU knockdown cells by qRT-PCR. β -Actin was used as a control. *ISCU_KD*, ISCU knockdown cell line; *NC*, control cell line. *, $p < 0.05$ compared with the control group. D, the predicted binding site for miR-210 at 3'-UTR of TfR gene is shown. The **bold font** shows the seed sequence of miR-210. E, MCF7 cells were co-transfected with pre-miR-210 or pre-NC and psi-TfR or with its mutant or deletion vector. After 48 h, luciferase activities were measured. *, $p < 0.05$ compared with pre-NC. *n.s.*, not significant. F, MCF7 cells were transfected with pre-miR-210 or pre-NC. After 48 h, transfected cells were incubated with Alexa Fluor 594-labeled Tf for 45 min. Expression of TfR (y axis) and uptake of transferrin (x axis) (upper panel) were analyzed by FACS. The right lower panel represents the expression of TfR. The left lower panel represents uptake of transferrin. Dashed histogram, transfected pre-NC; filled histogram, transfected pre-miR-210. G, MCF7 cells were transfected with pre-miR-210 or pre-NC. After 48 h, transfected cells were incubated with Alexa Fluor 594-labeled Tf (red) for 45 min and fixed in 4% paraformaldehyde for 30 min. Subsequently, cells were immunostained using anti-TfR antibody and an Alexa Fluor 488-conjugated secondary antibody (green). The nucleus was then stained with the Hoechst 33342 (blue). Scale bar, 50 μ m.

cancer cells. These results prompted us with the idea that iron-ISCU pathway might regulate the iron homeostasis in breast cancer cells.

miR-210 Suppresses the Major Iron-uptake Protein TfR—In mammalian cells, knockdown of ISCU markedly reduces mitochondrial aconitase activity and then promotes the activity of IRP1. Activation of IRP1 accelerates the binding to multiple iron-responsive elements in the 3'-UTR of the mRNA, such as TfR involved in iron acquisition, then leading to increased mRNA stability (26). When IRP1 binds to the 3'-UTR of TfR mRNA, which is an iron-uptake protein, the transcript is protected from degradation. Therefore, we hypothesized that overexpression of miR-210 stabilizes mRNA of TfR via the activation of IRP1. To prove this hypothesis, we measured the expression of mRNA and the protein level of TfR after transfection

of the miR-210 mimic (pre-miR-210) in MCF7 and MM231 cells. Surprisingly, the expression of TfR was down-regulated after the transfection of pre-miR-210 (Fig. 2, A and B, and supplemental Fig. S4A). This is an unexpected result because the expression of TfR was increased in ISCU stably knockdown cells (Fig. 2C and supplemental Fig. S2E). Those results led us to consider that miR-210 directly suppressed the expression of TfR by binding to the 3'-UTR of TfR. To check whether or not TfR is a direct target gene of miR-210, we once again used *in silico* algorithms and found that there was an miR-210-binding site at 3'-UTR of TfR (Fig. 2D). To prove that miR-210 directly recognizes the identical predicted target site in the 3'-UTR of TfR, MCF7 cells were transfected with psi-TfR, which was fused to 3'-UTR of TfR and the luciferase open reading frame, or a control vector. In addition, we also prepared

Regulation of Iron Homeostasis by miR-210

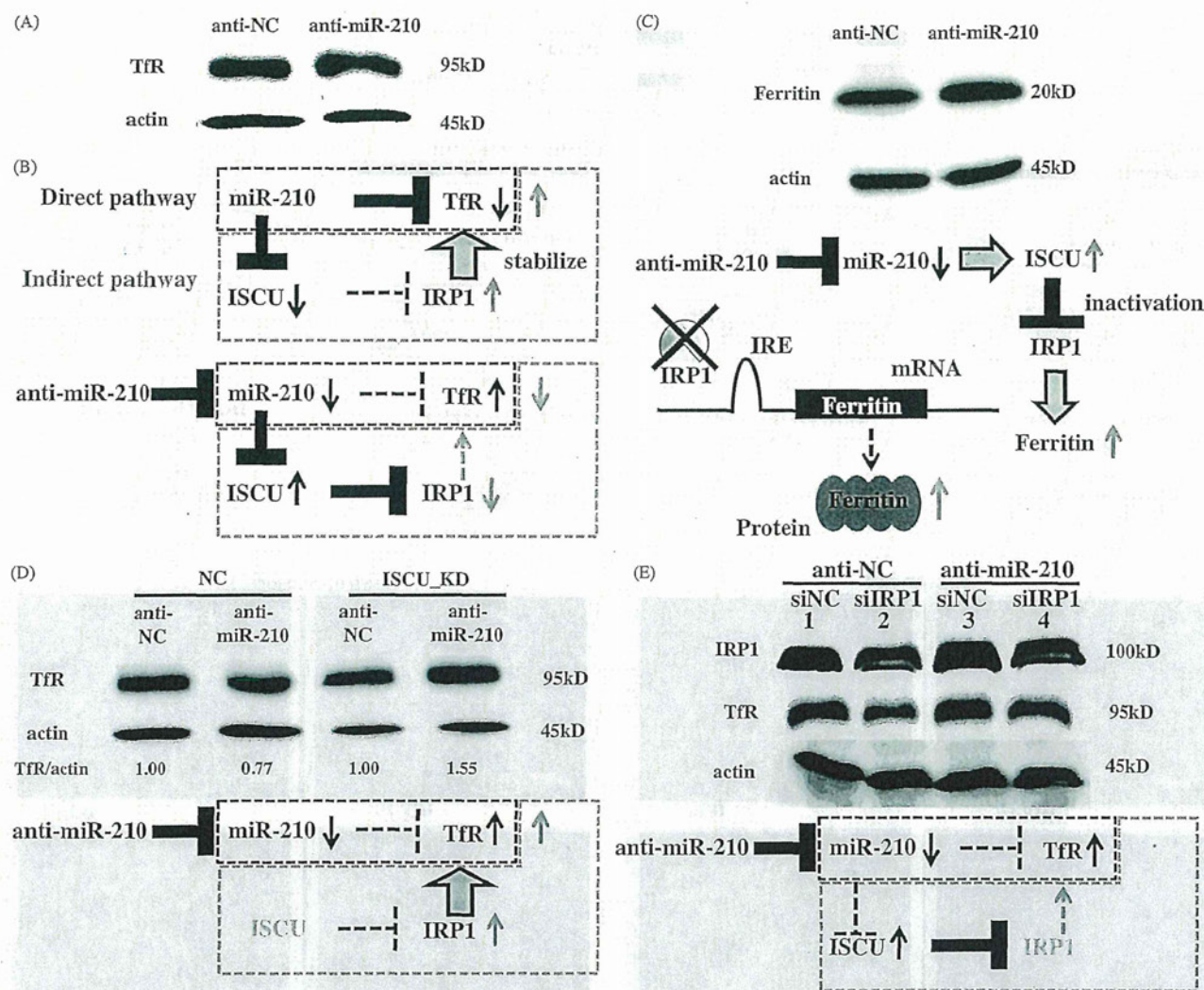


FIGURE 3. miR-210 has two pathways for regulating TfR expression. *A*, MCF7 cells were transfected with anti-miR-210 or anti-NC and exposed to 1% O₂ for 48 h. TfR expression was detected by immunoblotting. Actin was used as a loading control. *B*, schematic represents the regulation of two miR-210 target genes after treatment with anti-miR-210. After the transfection of anti-miR-210, the expression of TfR was indirectly decreased via the up-regulation of ISCU. On the other hand, the expression of TfR was directly increased through the down-regulation of miR-210. The expression of TfR then seemed to be unchanged after the transfection of anti-miR-210. **Direct pathway** means that miR-210 recognized the 3'-UTR of TfR and directly (see *black box*) regulates its expression. On the other hand, **Indirect pathway** means that miR-210 indirectly regulates TfR expression through the ISCU-IRP1 pathway (see *gray box*). After the transfection of anti-miR-210 (see *lower panel*), the expression of miR-210 was down-regulated, and then the expression of TfR was up-regulated (see *black box*). On the other hand, expression of ISCU was up-regulated after the transfection of anti-miR-210, and then the activity of IRP1 was inhibited by up-regulation of ISCU. IRP1 was important for the translation of TfR. Thus, inhibition of IRP1 activity by up-regulation of ISCU results in the down-regulation of TfR (see *gray box*). *C*, MCF7 cells were transfected with anti-miR-210 or anti-NC and exposed to 1% O₂. After 48 h, ferritin expression was detected by immunoblotting. Actin was used as a loading control. *Lower panel* shows schematic representation of the regulation of miR-210 target gene and ferritin after treatment with anti-miR-210. *D*, ISCU knockdown cell lines were transfected with anti-miR-210 or anti-NC and exposed to 1% O₂ for 48 h. TfR expression was detected by immunoblotting and quantified by densitometry. Actin was used as a loading control. *Lower panel* shows schematic representation of the regulation of miR-210 target gene after treatment with anti-miR-210 in ISCU_KD cells. Because ISCU was stably suppressed by shRNA in these cells, the activity of IRP1 was increased (*gray box*). Therefore, in this experiment, TfR was up-regulated by not only the down-regulation of miR-210 that directly targets the TfR but also the activation by IRP1. *E*, MCF7 cells were transfected with anti-miR-210 or anti-NC and siIRP1 or siNC and exposed to 1% O₂ for 48 h. Expression of IRP1 (*upper*) and TfR (*middle*) was detected by immunoblotting. Actin was used as a loading control. *Lower panel* shows schematic representation of the regulation of miR-210 target gene after treatment with anti-miR-210 and siIRP1. Because the expression of IRP1 was suppressed by siRNA, there is no influence on the TfR expression by *Indirect pathway* (*gray box*). On the other hand, the expression of miR-210 was down-regulated by anti-miR-210. As a result, TfR was up-regulated in this experiment.

psi-TfR_mut, which has a mutated sequence of a putative miR-210-binding site or psi-TfR_del, which has deleted a putative miR-210-binding site. Co-transfection of pre-miR-210 down-regulated *Renilla* luciferase activity significantly more than in pre-NC in the presence of psi-TfR. In contrast, *Renilla* luciferase activity was not altered in the presence of psi-TfR_del or psi-TfR_mut (Fig. 2E). We confirmed that miR-210 targets the 3'-UTR of TfR mRNA, showing that miR-210 directly sup-

presses not only ISCU but also TfR. TfR plays a major role in cellular iron uptake through binding to and internalizing a carrier protein transferrin (Tf). Therefore, to examine whether reduction of TfR by transfected pre-miR-210 functionally inhibited the uptake of Tf or not, Alexa Fluor 594-labeled Tf was used to monitor the uptake of Tf by immunostaining and FACS analysis. As shown in Fig. 2, F and G, uptake of Tf was lower in pre-miR-210-transfected cells than in control cells,

Regulation of Iron Homeostasis by miR-210

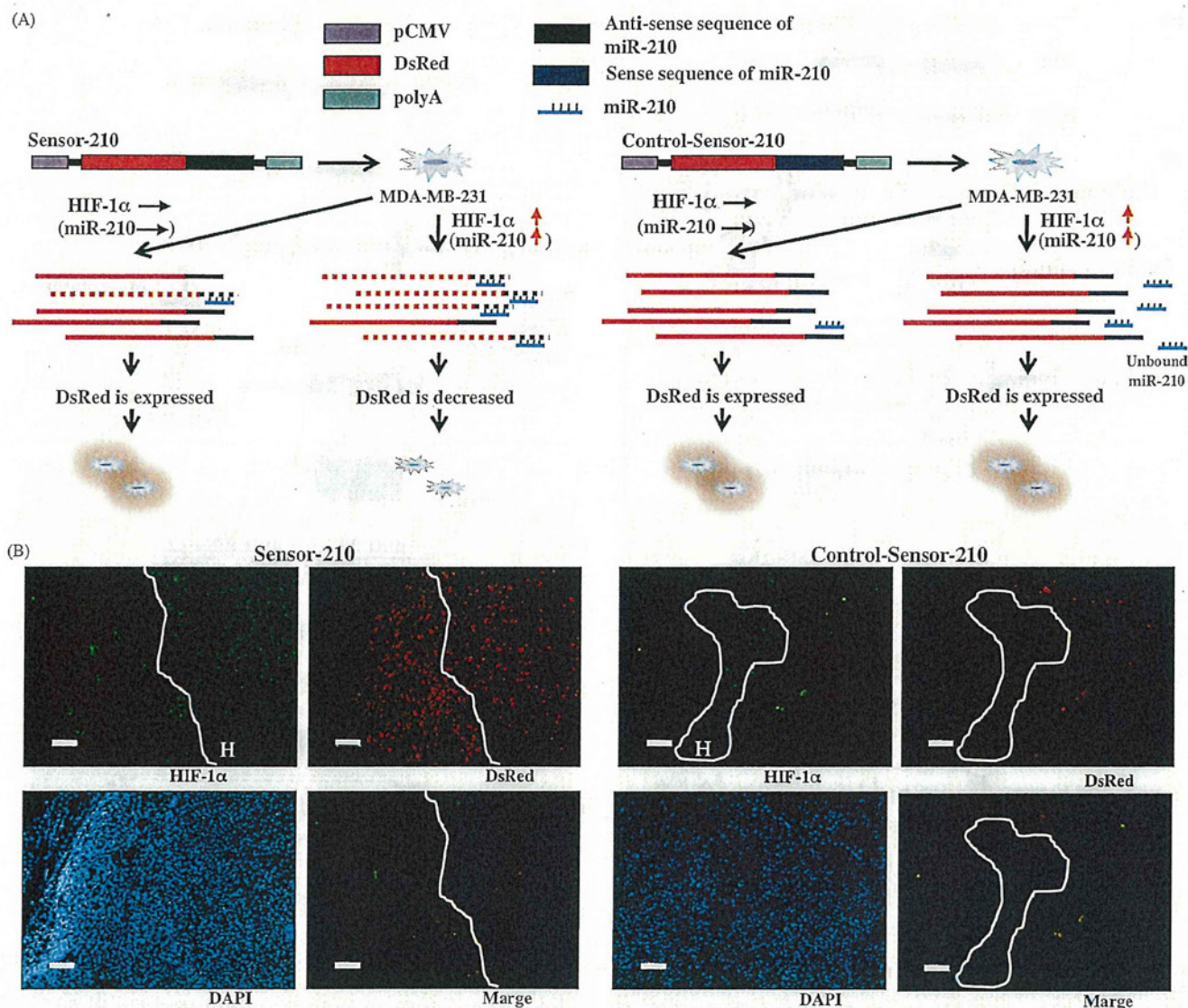


FIGURE 4. miR-210-expressing cells were localized in the chronic hypoxic region of inoculated tumor cells. *A*, schematic represents miR-210 tracing assay. In the hypoxic condition, expression of miR-210 is increased by the HIF-1, and then the transcripts of DsRed are degraded by miR-210 (dashed lines with red and black). On the other hand, expression of miR-210 is not changed under the normoxic condition (lines with red and black). In addition, the fluorescence of Control-Sensor-210 was not changed even under hypoxic conditions. Because their miR-210-binding sites were inserted inversely, the miR-210 could not bind to the 3'-UTR of DsRed. *B*, immunohistochemical analysis of DsRed in the tumor is shown. Sections were stained with the rabbit polyclonal anti-red fluorescent protein antibody and the mouse monoclonal anti-HIF-1 α antibody. The fluorescence of DsRed could not be observed in HIF-1 α -positive regions in the Sensor-210-inoculated tumor; on the other hand, there was uniform fluorescence of DsRed in Control-Sensor-210-cells-inoculated tumor. *H*, hypoxic region in a tumor is indicated. Scale bar, 100 μ m.

indicating a direct correlation between TfR reduction and the decreased uptake of Tf in miR-210-overexpressing cells (Fig. 2, *F* and *G*). We also confirmed similar results using an MM231 cells (supplemental Fig. S4, *B* and *C*). Consequently, these observations indicated that overexpression of miR-210 decreases the concentration of intracellular iron by inhibiting the Tf-TfR-dependent iron-uptake system.

miR-210 Is a Member of Iron Homeostatic Networks—As shown in Fig. 2, overexpression of miR-210 inhibited the uptake of Tf via the suppression of TfR. However, because overexpression of miR-210 by miR-210 mimics transduces an extremely high amount of miRNA in the cells (supplemental Fig. S3A), it is necessary to examine the function of miR-210 in iron homeostasis under physiological conditions. To evaluate the physio-

logical relationship among miR-210, ISCU, and TfR expression, we transfected antisense miR-210 oligonucleotide (anti-miR-210), which suppresses the expression of miR-210 (supplemental Fig. S3B) and control oligonucleotide (anti-NC) into MCF7 cells under a hypoxic condition. We observed the induction of ISCU expression level after the transfection of anti-miR-210 (Fig. 1*F* and supplemental Fig. S2*D*); however, the expression of TfR was not affected (Fig. 3*A* and supplemental Fig. S5*A*). The knockdown of ISCU has been known to increase the expression of TfR by activating IRP1 activity (Fig. 2*C*) (26). From these observations, we assumed that unchanged TfR expression after the transfection of anti-miR-210 was caused by the up-regulation of the ISCU expression level by anti-miR-210 (Fig. 3*B*), leading to the inhibition of IRP1 activity without affecting the

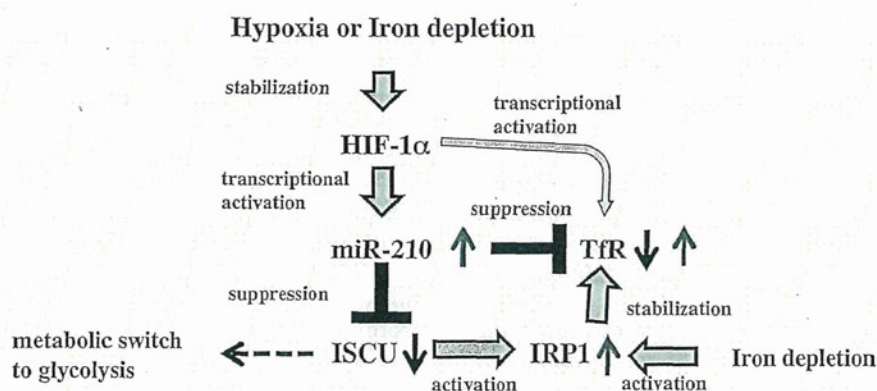


FIGURE 5. Schematic representation of our proposed model. miR-210 is induced by hypoxia and iron depletion and directly suppresses two iron homeostasis-related proteins. miR-210 regulates the iron homeostasis with dual pathways of regulating Tfr expression. The gray arrows indicate up-regulation, and the black arrows indicate down-regulation. The dashed arrow indicates shift to metabolic switch.

IRP1 expression level. To confirm the change of IRP1 activity by miR-210 expression level in our experiment, we transfected anti-miR-210 or pre-miR-210 into MCF7 cells and analyzed the expression level of ferritin protein, which is the iron storage protein, by immunoblotting. Because the 5'-UTR of ferritin mRNA contains a single iron-responsive element that affects translation initiation, inhibition of IRP1 activity led to the up-regulation of ferritin expression (29). Indeed, the expression level of ferritin was increased in anti-miR-210-transfected cells compared with that in anti-NC-transfected cells (Fig. 3C). On the other hand, overexpression of miR-210 by pre-miR-210 suppressed the expression of ferritin in MCF7 cells, indicating that the activity of IRP1 was modulated by miR-210 through ISCU pathway (supplemental Fig. S5B). To eliminate the effect of ISCU on Tfr expression in this assay system, we established stable ISCU knockdown cell lines using the MCF7 cell. In ISCU knockdown cells, the expression of Tfr was higher than that in control cells by activated IRP1 (Fig. 2C and supplemental Fig. S2E). We carried out the same experiment as shown in Fig. 3A using ISCU knockdown cell lines and observed that anti-miR-210 increased Tfr mRNA and protein level in ISCU knockdown cell lines but not in control cell lines (Fig. 3D). This result indicated that the expression of Tfr was up-regulated by not only the down-regulation of miR-210 that directly target the Tfr but also the activated IRP1, which is usually inactivated by ISCU. Furthermore, MCF7 cells were transfected with siRNA against IRP1 (or siNC) and anti-miR-210 (or anti-NC) under hypoxic condition, and these cells were analyzed for the expression of IRP1 and Tfr by immunoblotting. As a result, because the IRP1 is known to stabilize the Tfr mRNA, knockdown of IRP1 by siRNA caused a decrease in the expression of Tfr (Fig. 3E; compare lanes 1 and 2). Importantly, co-transfection of anti-miR-210 and IRP1 siRNA induced the expression of Tfr, indicating that miR-210 directly targets the Tfr in cancer cells (Fig. 3E; compare lanes 2 and 4). Taken together, these data suggest that miR-210 regulates Tfr expression through direct and indirect translational regulatory mechanisms to fine-tune the iron homeostasis (Fig. 3B).

The Distribution of miR-210-expressing Cells Is Associated with Chronic Hypoxia—Most tumors have lower median O_2 partial pressures than their tissue of origin and are deprived of nutrients, including iron (30). Significant variations in these relevant parameters must be expected between different locations within the same tumor at the same location at different times and between individual tumors of the same grading and staging. Previous results have shown that the expression of miR-210 is modulated by the cellular iron concentration and oxygen tension; however, what kinds of cells *in vivo* expressed miR-210 have not been clarified yet. For this reason, we postulated that clarifying the distribution of miR-210-expressing cells in the tumor leads to the understanding of cancer metabolism regulated by iron concentration. To answer this, we investigated the distribution of miR-210-expressing cells in an *in vivo* breast tumor xenograft model. In this experiment, we prepared the cell line, called MDA-MB-231-miR-210-sensor, to trace the expression of miRNA-210 *in vivo*. Because this cell was established by DsRed harboring a complementary sequence of miR-210, the fluorescence of DsRed was diminished when the expression of miR-210 was induced (Fig. 4A and supplemental Fig. S6A). We injected 5×10^6 MDA-MB-231-miR-210-sensor cells into nude mice. Prior to the excision of tumors, the mice were administered pimonidazole, a compound that binds irreversibly to hypoxic cells (31). Serial sections of the tumors were subsequently stained for pimonidazole, HIF-1 α , and DsRed. A correlation between HIF-1 α -positive cells and DsRed-negative cells, indicative of diminishment of DsRed expression by miR-210, was observed at the hypoxic rim around necrotic regions of the tumor, a location typically associated with chronic hypoxia (Fig. 4B). We also observed that pimonidazole-positive cells and DsRed-negative cells overlapped. On the other hand, fluorescence of control-miR-210-sensor cells, whose miR-210-binding site was inserted inversely with the miR-210-sensor vector, was not changed in inoculated tumor cells. Furthermore, we also established a cell line that enabled us to trace the expression of miR-210 by its promoter-driven DsRed (Fig. S6B) and obtained similar results with the MDA-MB-231-miR-210-sensor (Fig. S6C). Together, these observations indicated that the expression of miR-210 was

Regulation of Iron Homeostasis by miR-210

increased in the severely hypoxic region of the tumor. Namely, miR-210 regulates the iron homeostasis in cancer cells under the chronic hypoxic condition in tumors.

DISCUSSION

Iron is indispensable for the function of many prosthetic groups, whereas excess free iron can oxidize and damage the protein, nucleic acid, and lipid contents of cells. Thus, animals evolved complex mechanisms to control the favorable concentrations of intracellular iron. In this study, we revealed that miR-210 is involved in a novel iron homeostasis mechanism through the association of ISCU and Tfr in cancer cells (Fig. 5). miR-210 down-regulates ISCU and the Fe-S cluster to mediate the energy metabolic shift from aerobic oxidative phosphorylation to anaerobic glycolysis (32). Concurrently, reduction of the Fe-S cluster activates IRP1, and, subsequently, the expression of Tfr is increased, resulting in the elevated uptake of the iron ion. However, several reports show that the excess iron can be toxic (4). To reduce the cellular iron concentration, miR-210 directly suppresses the expression of Tfr. Thus, miR-210 regulates iron homeostasis and avoids intracellular iron toxicity.

Compared with normal cells, cancer cells require a large amount of iron; thus, they generally proliferate at a larger rate than their normal counterparts. Hence, iron chelators exert their anti-proliferative effects on tumors (12). Moreover, a previous report showed that down-regulation of Tfr decreased cellular proliferation and altered expression of genes involved in cell cycle control (33). Thus, as summarized in Fig. 5, it is postulated that miR-210 has two pathways for the regulation of Tfr expression. One is the Tfr up-regulation pathway via suppression of ISCU (indirect pathway), and the other one is the Tfr down-regulation pathway by direct binding to Tfr mRNA. Reduction of ISCU only increases the binding activity of IRP1, but its level of expression does not change. Thus, the effect of up-regulation of Tfr by reduced ISCU depends on the amount of IRP1 protein. There are limitations to the up-regulation of Tfr by the indirect pathway. Then, in the case of a further increase of miR-210, direct suppression of Tfr is superior to its up-regulation by the indirect pathway. In other words, because the forced expression of miR-210 overwhelms the indirect pathway, the direct pathway is superior to the indirect one. Therefore, exogenous transfection of miR-210 causes Tfr suppression (Fig. 2), thereby reducing cellular proliferation (supplemental Fig. S7) (34, 35). Moreover, we confirmed the overlap of chronic hypoxic regions and miR-210-expressing cells in inoculated cancer cells *in vivo*. These observations suggest that precise regulation of miR-210 expression level is vital for maintaining the iron homeostasis, leading to the survival and proper cellular proliferation of cancer cells.

HIFs and IRPs are key mediators of cellular iron homeostasis and oxygen, respectively. Because iron and oxygen are often intimately connected in their metabolism, it is not surprising that their levels are coordinately regulated in cells. Such cross-talk is achieved in part by cellular regulatory factors that sense and respond to both iron and oxygen, and it is reinforced by the overlap in the gene targets regulated by each pathway. For instance, binding of IRPs protects Tfr mRNA from degradation, and HIF-1 α activates Tfr gene transcription (36, 37). In

addition, in this study, we identified that hypoxia-inducible miR-210 was a key component of this pathway.

As noted above, we have clearly shown that iron homeostasis is micromanaged by miRNAs. Therefore, miRNAs could be essential for maintaining other metal homeostasis in mammals; for example, copper, zinc, and cadmium. In agreement with our observations, the current view on the molecular understanding of miRNA-guided regulation of plant heavy metal adaptation was reported (38, 39). Dysregulation of metal homeostasis-related miRNAs may contribute to various diseases including cancers, nephropathy, and autoimmune disease. Further analyses are required on how these miRNAs can be affected by genetic and epigenetic mechanisms in the physiological and pathological microenvironments.

Acknowledgments—We thank Haruhisa Iguchi and Ryou-u Takahashi for participation in discussions and technical advice, Yusuke Yamamoto for participation in helpful discussions, Ayako Inoue, and Keitaro Hagiwara for excellent technical assistance.

REFERENCES

1. Que, L., Jr., and Ho, R. Y. (1996) Dioxygen activation by enzymes with mononuclear nonheme iron active sites. *Chem. Rev.* **96**, 2607–2624
2. Pau, M. Y., Lipscomb, J. D., and Solomon, E. I. (2007) Substrate activation for O₂ reactions by oxidized metal centers in biology. *Proc. Natl. Acad. Sci. U.S.A.* **104**, 18355–18362
3. Hegg, E. L., and Que, L., Jr. (1997) The 2-His-1-carboxylate facial triad: an emerging structural motif in mononuclear nonheme iron(II) enzymes. *Eur. J. Biochem.* **250**, 625–629
4. Stadtman, E. R. (1990) Metal ion-catalyzed oxidation of proteins: biochemical mechanism and biological consequences. *Free Radic. Biol. Med.* **9**, 315–325
5. Clark, S. F. (2009) Iron-deficiency anemia: diagnosis and management. *Curr. Opin. Gastroenterol.* **25**, 122–128
6. Raja, K. B., Duane, P., and Peters, T. J. (1990) Effects of turpentine-induced inflammation on the hypoxic stimulation of intestinal Fe³⁺ absorption in mice. *Int. J. Exp. Pathol.* **71**, 785–789
7. Laftah, A. H., Raja, K. B., Latunde-Dada, G. O., Vergi, T., McKie, A. T., Simpson, R. J., and Peters, T. J. (2005) Effect of altered iron metabolism on markers of haem biosynthesis and intestinal iron absorption in mice. *Ann. Hematol.* **84**, 177–182
8. Peyssonnaud, C., Zinkernagel, A. S., Schuepbach, R. A., Rankin, E., Vaulont, S., Haase, V. H., Nizet, V., and Johnson, R. S. (2007) Regulation of iron homeostasis by the hypoxia-inducible transcription factors (HIFs). *J. Clin. Invest.* **117**, 1926–1932
9. Wang, G. L., Jiang, B. H., Rue, E. A., and Semenza, G. L. (1995) Hypoxia-inducible factor 1 is a basic-helix-loop-helix-PAS heterodimer regulated by cellular O₂ tension. *Proc. Natl. Acad. Sci. U.S.A.* **92**, 5510–5514
10. Wang, G. L., and Semenza, G. L. (1995) Purification and characterization of hypoxia-inducible factor 1. *J. Biol. Chem.* **270**, 1230–1237
11. Campbell, J. A. (1940) Effects of precipitated silica and of iron oxide on the incidence of primary lung tumors in mice. *Br. Med. J.* **2**, 275–280
12. Richardson, D. R., Kalinowski, D. S., Lau, S., Jansson, P. J., and Lovejoy, D. B. (2009) Cancer cell iron metabolism and the development of potent iron chelators as anti-tumor agents. *Biochim. Biophys. Acta* **1790**, 702–717
13. Bartel, D. P. (2004) MicroRNAs: genomics, biogenesis, mechanism, and function. *Cell* **116**, 281–297
14. Stefani, G., and Slack, F. J. (2008) Small noncoding RNAs in animal development. *Nat. Rev. Mol. Cell Biol.* **9**, 219–230
15. Calin, G. A., and Croce, C. M. (2006) MicroRNA signatures in human cancers. *Nat. Rev. Cancer* **6**, 857–866
16. Rasmussen, K. D., Simmini, S., Abreu-Goodger, C., Bartonicek, N., Di Giacomo, M., Bilbao-Cortes, D., Horos, R., Von Lindern, M., Enright, A. J.,

- and O'Carroll, D. (2010) The miR-144/451 locus is required for erythroid homeostasis. *J. Exp. Med.* **207**, 1351–1358
17. Kosaka, N., Sugiura, K., Yamamoto, Y., Yoshioka, Y., Miyazaki, H., Komatsu, N., Ochiya, T., and Kato, T. (2008) Identification of erythropoietin-induced microRNAs in haematopoietic cells during erythroid differentiation. *Br. J. Haematol.* **142**, 293–300
 18. Camps, C., Buffa, F. M., Colella, S., Moore, J., Sotiriou, C., Sheldon, H., Harris, A. L., Gleadly, J. M., and Ragoussis, J. (2008) HSA-miR-210 is induced by hypoxia and is an independent prognostic factor in breast cancer. *Clin. Cancer Res.* **14**, 1340–1348
 19. Friedman, R. C., Farh, K. K., Burge, C. B., and Bartel, D. P. (2009) Most mammalian mRNAs are conserved targets of microRNAs. *Genome Res.* **19**, 92–105
 20. Griffiths-Jones, S., Grocock, R. J., van Dongen, S., Bateman, A., and Enright, A. J. (2006) miRBase: microRNA sequences, targets, and gene nomenclature. *Nucleic Acids Res.* **34**, D140–144
 21. Wang, X., and El Naqa, I. M. (2008) Prediction of both conserved and nonconserved microRNA targets in animals. *Bioinformatics* **24**, 325–332
 22. Huang, X., Ding, L., Bennewith, K. L., Tong, R. T., Welford, S. M., Ang, K. K., Story, M., Le, Q. T., and Giaccia, A. J. (2009) Hypoxia-inducible miR-210 regulates normoxic gene expression involved in tumor initiation. *Mol. Cell* **35**, 856–867
 23. Fujita, S., Ito, T., Mizutani, T., Minoguchi, S., Yamamichi, N., Sakurai, K., and Iba, H. (2008) miR-21 gene expression triggered by AP-1 is sustained through a double-negative feedback mechanism. *J. Mol. Biol.* **378**, 492–504
 24. Burk, U., Schubert, J., Wellner, U., Schmalhofer, O., Vincan, E., Spaderna, S., and Brabletz, T. (2008) A reciprocal repression between ZEB1 and members of the miR-200 family promotes EMT and invasion in cancer cells. *EMBO Rep.* **9**, 582–589
 25. Ye, H., and Rouault, T. A. (2010) Erythropoiesis and iron-sulfur cluster biogenesis. *Adv. Hematol.* **2010**, 10.1155/2010/329394
 26. Tong, W. H., and Rouault, T. A. (2006) Functions of mitochondrial ISCU and cytosolic ISCU in mammalian iron-sulfur cluster biogenesis and iron homeostasis. *Cell Metab.* **3**, 199–210
 27. Chen, Z., Li, Y., Zhang, H., Huang, P., and Luthra, R. (2010) Hypoxia-regulated microRNA-210 modulates mitochondrial function and decreases ISCU and COX10 expression. *Oncogene* **29**, 4362–4368
 28. Favaro, E., Ramachandran, A., McCormick, R., Gee, H., Blancher, C., Crosby, M., Devlin, C., Blick, C., Buffa, F., Li, J. L., Vojnovic, B., Pires das Neves, R., Glazer, P., Iborra, F., Ivan, M., Ragoussis, J., and Harris, A. L. (2010) MicroRNA-210 regulates mitochondrial free radical response to hypoxia and Krebs cycle in cancer cells by targeting iron-sulfur cluster protein ISCU. *PLoS One* **5**, e10345
 29. Hentze, M. W., Caughman, S. W., Rouault, T. A., Barriocanal, J. G., Dancis, A., Harford, J. B., and Klausner, R. D. (1987) Identification of the iron-responsive element for the translational regulation of human ferritin mRNA. *Science* **238**, 1570–1573
 30. Vaupel, P., Kallinowski, F., and Okunieff, P. (1989) Blood flow, oxygen and nutrient supply, and metabolic microenvironment of human tumors: a review. *Cancer Res.* **49**, 6449–6465
 31. Raleigh, J. A., Chou, S. C., Arteel, G. E., and Horsman, M. R. (1999) Comparisons among pimonidazole binding, oxygen electrode measurements, and radiation response in C3H mouse tumors. *Radiat. Res.* **151**, 580–589
 32. Chan, S. Y., Zhang, Y. Y., Hemann, C., Mahoney, C. E., Zweier, J. L., and Loscalzo, J. (2009) MicroRNA-210 controls mitochondrial metabolism during hypoxia by repressing the iron-sulfur cluster assembly proteins ISCU1/2. *Cell Metab.* **10**, 273–284
 33. O'Donnell, K. A., Yu, D., Zeller, K. I., Kim, J. W., Racke, F., Thomas-Tikhonenko, A., and Dang, C. V. (2006) Activation of transferrin receptor 1 by c-Myc enhances cellular proliferation and tumorigenesis. *Mol. Cell Biol.* **26**, 2373–2386
 34. Chitambar, C. R., Massey, E. J., and Seligman, P. A. (1983) Regulation of transferrin receptor expression on human leukemic cells during proliferation and induction of differentiation: effects of gallium and dimethylsulfoxide. *J. Clin. Invest.* **72**, 1314–1325
 35. Neckers, L. M., and Trepel, J. B. (1986) Transferrin receptor expression and the control of cell growth. *Cancer Invest.* **4**, 461–470
 36. Lok, C. N., and Ponka, P. (1999) Identification of a hypoxia-response element in the transferrin receptor gene. *J. Biol. Chem.* **274**, 24147–24152
 37. Tacchini, L., Bianchi, L., Bernelli-Zazzera, A., and Cairo, G. (1999) Transferrin receptor induction by hypoxia: HIF-1-mediated transcriptional activation and cell-specific post-transcriptional regulation. *J. Biol. Chem.* **274**, 24142–24146
 38. Yamasaki, H., Abdel-Ghany, S. E., Cohu, C. M., Kobayashi, Y., Shikanai, T., and Pilon, M. (2007) Regulation of copper homeostasis by microRNA in *Arabidopsis*. *J. Biol. Chem.* **282**, 16369–16378
 39. Abdel-Ghany, S. E., and Pilon, M. (2008) MicroRNA-mediated systemic down-regulation of copper protein expression in response to low copper availability in *Arabidopsis*. *J. Biol. Chem.* **283**, 15932–15945

